Applied Catalysis B: Environmental 194 (2016) 32–41

Contents lists available at ScienceDirect

Applied Catalysis B: Environmental

journal homepage: www.elsevier.com/locate/apcatb

Comparative study on the removal of humic acids from drinking water by anodic oxidation and electro-Fenton processes: Mineralization efficiency and modelling

Clément Trellu[a], Yoan Péchaud[a], Nihal Oturan[a], Emmanuel Mousset[a], David Huguenot[a], Eric D. van Hullebusch[a], Giovanni Esposito[b], Mehmet A. Oturan[a,*]

[a] Université Paris-Est, Laboratoire Géomatériaux et Environnement (EA 4508), UPEM, 77454 Marne-la-Vallée, France
[b] University of Cassino and the Southern Lazio, Department of Civil and Mechanical Engineering, Via Di Biasio, 43, 03043 Cassino, Frosinone, Italy

ARTICLE INFO

Article history:
Received 1 March 2016
Received in revised form 12 April 2016
Accepted 19 April 2016
Available online 22 April 2016

Keywords:
Humic acid
Anodic oxidation
Electro-Fenton
BDD anode
Carbon sponge
Adsorption
Modelling

ABSTRACT

The management of natural organic matter in drinking water treatment plants is an important matter of concern. It can generate toxic disinfection by-products as well as decrease the efficiency of membrane filtration and oxidation processes. This is the first study that investigates the use of anodic oxidation (AO) and electro-Fenton (EF) for the removal of humic acids (HAs) from aqueous solutions. Both sorption and catalytic oxidation of HAs are assessed and discussed. These electrochemical advanced oxidation processes are based on the *in situ* production of hydroxyl radicals, a highly oxidizing agent. The EF process involves the use of carbon-based porous materials (carbon sponge) as cathode, leading to the fast adsorption of hydrophobic HAs. It has been observed that adsorbed HAs can react with hydroxyl radical produced in the bulk from Fenton's reaction. Then, the release in the solution of more hydrophilic by-products from the oxidation of HAs leads to a rebound effect of the organic matter concentration. Therefore, the AO process using non-carbonaceous cathode materials appears to be more suitable for HAs removal. Using boron-doped diamond anode and stainless steel cathode, the mineralization efficiency of a HAs solution (TOC_0 = 16.2 mg L^{-1}) reached more than 99% after 7 h of AO treatment with a current intensity of 1000 mA. By considering both sorption and oxidation processes, this study proposed a new modelling approach to monitor TOC evolution during AO and EF processes.

© 2016 Elsevier B.V. All rights reserved.

1. Introduction

Humic substances (HS) are major components of the natural organic matter (NOM) in soil and water. They are complex and heterogeneous mixtures of polydispersed materials formed by biochemical and chemical reactions during humification of plant and microbial remains [1]. The major extractable component of HS in peat and grassland soils is humic acids (HAs) (70–80%) [2]. They are complex aromatic macromolecules containing phenolic groups, quinone structures, aliphatic compounds, nitrogen and oxygen as bridge units and carboxylic groups variously placed on aromatic rings [1,2].

HS are non-toxic compounds, but they have a significant influence on selection, design and operation of water treatment processes. The greatest concern is their precursor role in the formation of highly toxic disinfection by-products such as trihalomethanes [3–5]. NOM can be removed from drinking water by several treatment options. The most common and economically feasible process is considered to be coagulation and flocculation followed by decantation and sand filtration [6]. Concentrations of dissolved organic carbon can range from 0.1 mg L^{-1} in groundwater to 50 mg L^{-1} in bogs [7]. These concentrations depend on the nature of the watershed, but are also strongly influenced by seasonal variations and particulate organic carbon inputs such as runoff or algae bloom [7]. Therefore, the increased requirements in drinking water quality lead to invest additional methods for NOM removal. The following methods can constitute alternative processes: advanced oxidation processes (AOPs) [8,9], ozonation [10], sonolysis [11] or UV-based processes [12]. However, the preferential degradation

Abbreviations: AO, anodic oxidation; BDD, boron doped diamond; CS, carbon sponge; EAOPs, electrochemical advanced oxidation processes; EF, electro-Fenton; HAs, humic acids; HA_{ads}, humic acids adsorbed; HA_{hob}, low or non-degraded humic acids; HA_{hob_ads}, low or non-degraded humic acids adsorbed; HA_{tot}, total humic acids; IoA, index of agreement; ME, model efficiency; TOC_{sol}, TOC in the solution; TOC_{ads}, TOC adsorbed; RMSE, root mean square error; SS, stainless steel.

* Corresponding author.
E-mail address: mehmet.oturan@univ-paris-est.fr (M.A. Oturan).

http://dx.doi.org/10.1016/j.apcatb.2016.04.039
0926-3373/© 2016 Elsevier B.V. All rights reserved.

of hydrophobic organic compounds has been observed in many studies. Moreover, incomplete oxidation can lead to increase the potential of formation of disinfection by-products [8].

Electrochemical advanced oxidation processes (EAOPs) are new attractive techniques for water treatment [13–20]. They are based on the *in situ* generation of hydroxyl radicals (•OH), the second strongest oxidizing agent known [21]. Their high efficiency for the removal of a large range of persistent organic pollutants (POPs) with complete mineralization to CO_2 has already been shown [22–29]. However, NOM can reduce removal efficiency, due to complexation with POPs as well as •OH scavenging [30]. The management of NOM is also crucial for the treatment strategy combining EAOPs and membrane processes because it is the main responsible of membrane fouling [31,32].

Hydroxyl radicals react with a wide spectrum of NOM of both hydrophobic and hydrophilic character. Rate constants for reactions with NOM have been measured at $1–5 \times 10^8\ M^{-1}\ s^{-1}$ [33]. One of the most popular EAOPs is anodic oxidation (AO) process in which organic compounds directly react with heterogeneous hydroxyl radicals M(•OH) [34], formed by oxidation of water at the surface of anodes (M) with high oxygen overpotential [35,36] (Eq. (1)). Particularly, boron doped diamond (BDD) anode has very high catalytic activity and allows producing large amount of hydroxyl radicals.

$$M + H_2O \rightarrow M(^{\bullet}OH) + H^+ + e^- \quad (1)$$

The other popular EAOPs is the electro-Fenton (EF) process, in which •OH are produced homogeneously in the bulk of treated solution from the electrochemically generated Fenton's reagent (mixture of H_2O_2 and Fe^{2+}) [37–40] (Eq. (2)). H_2O_2 is *in situ* electrogenerated at the cathode following Eq. (3) from two-electrons reduction of dissolved O_2 [17,40]. A catalytic amount of ferrous iron salt is sufficient to turn up the process, due to the catalytic electro-regeneration of ferrous iron at the cathode (Eq. (4)) [41–43].

$$Fe^{2+} + H_2O_2 \rightarrow Fe^{3+} + {}^{\bullet}OH + OH^- \left(k = 63 M^{-1}s^{-1}\right) \quad (2)$$

$$O_2 + 2H^+ + 2e^- \rightarrow H_2O_2 \quad (3)$$

$$Fe^{3+} + e^- \rightarrow Fe^{2+} \quad (4)$$

These formed homogeneous/heterogeneous •OH can then react with the organic matter (R) to oxidize it until ultimate oxidation state is reached, i.e., mineralization (Eq. (5)):

$$R + {}^{\bullet}OH/M(OH) \rightarrow M + CO_2 + H_2O + \text{mineralions} \quad (5)$$

To the best of our knowledge, it is the first time that the following processes are studied for removal of HAs: AO using BDD anode, EF using Platinum (Pt) anode, and EF using BDD anode. Carbon sponge (CS) was used as cathode, since it produces high amount of H_2O_2 for the EF process [44]. Stainless steel (SS) and CS were also compared as cathode material for the AO process. Sorption of HAs onto CS cathode was highlighted and the impact of this phenomenon on the electrocatalytic oxidation of HAs was assessed. Therefore the goal of this study was (i) to show the ability of EAOPs for total removal of HAs from water (ii) to assess and compare the effectiveness of various EAOPs for removal of HAs from aqueous solutions (iii) to understand HAs removal mechanisms during EAOPs (iv) to propose a new modeling approach to monitor TOC removal by taking into account both sorption and oxidation processes.

2. Material and methods

2.1. Chemicals

HAs were purchased from Acros Organics. A purification step was performed as described below. Iron(II) sulphate heptahydrated and sulphuric acid were of reagent grade obtained from Acros Organics. Sodium sulphate was of reagent grade purchased from Sigma Aldrich. Solutions were prepared with ultrapure water from a Millipore Milli-Q system (Molsheim, France) with resistivity > 18 MΩ cm.

2.2. Preparation of humic acid solutions

A purification step of commercial HAs was performed, similarly to the protocol of Arai et al. [45]. The stock solution was prepared by dissolving 1 g of commercial HAs in 2 L of Milli-Q water at pH 3. This solution was filtered through Whatman GF/F filter (0.7 μm as pore diameter). Then, HAs were precipitated by decreasing pH at 1.2 and the solution was centrifuged at 3000 rpm during 20 min. Supernatant was then removed and precipitated HAs were dissolved in deionized water and stocked at pH 3.

2.3. Electrochemical treatments

All electrochemical treatments were carried out during 9 h in a 400 mL batch electrochemical cell containing 330 mL of HAs solution at initial TOC concentration of 16.2 mg L^{-1} (TOC_0). The anode material was Pt ($14\ cm^2 \times 0.1$ cm) from Platecxis (Noisy-le-Sec, France) or a BDD thin-film onto a Nb substrate ($24\ cm^2 \times 0.2$ cm) purchased from Condias Gmbh (Itzehoe, Germany). The cathode material was CS ($24\ cm^2 \times 1.2$ cm, 60 pores per inch) from Magneto BV Holland (The Netherlands) or SS ($24\ cm^2 \times 0.2$ cm) from Goodfellow (France). Electrodes were set up with a gap of 3 cm between the anode and the cathode. The constant current intensity was provided by a power supply (HAMEG, Germany (model 7042-5)). Air was continuously bubbled inside the solution through a glass frit in order to keep enough dissolved oxygen in the solution for the hydrogen peroxide production at the cathode following Eq. (3). A magnetic stirrer ensured the homogenization of the solution in the electrochemical cell. Similarly to optimal experimental conditions determined by Özcan et al. [44], a suitable amount of electrolyte was dissolved in the solution (Na_2SO_4 at 0.05 M) and pH was adjusted at 3.0 with 1 M H_2SO_4. For EF process, an optimal concentration of 0.1 mM Fe^{2+} (under the form of ferrous sulphate heptahydrated) was added [44]. According to the electrochemical cell configuration, processes were denoted as AO-SS (BDD anode, SS cathode), AO-CS (BDD anode, CS cathode), EF-Pt (Pt anode, CS cathode, 0.1 mM Fe^{2+}) and EF-BDD (BDD anode, CS cathode, 0.1 mM Fe^{2+}).

2.4. Analytical procedures

Due to the complexity of the HAs mixture, organic matter content concentration was determined by a global parameter, i.e. the total organic carbon (TOC) content of the solution (TOC_{sol}), in mg L^{-1}. Samples (3.5 mL) were collected at 8 or 9 different time points during the electrolysis. TOC was measured by using a Shimadzu TOC-V analyzer. Calibration was achieved with potassium hydrogen phthalate (99.5%, Merck).

For the analytic determination of organics adsorbed onto the CS cathode (TOC_{ads}), the treated solution was removed from the electrochemical cell. Then, 330 mL of NaOH at 0.1 M was used for desorption of HAs from the cathode, similarly to the extraction method of HAs from soil [46]. After 15 min of continuous stirring, a sample was analysed after inorganic carbon removal from the solution by decreasing the pH at 3 and purging the sample with O_2 gas. Values were given in mg L^{-1}, based on the amount of carbon adsorbed on the cathode compared to the volume of the solution treated. Therefore, the total TOC (TOC_{tot}) in the solution was deduced as $TOC_{tot} = TOC_{sol} + TOC_{ads}$.

The evolution of the UV spectrum of the solution and compounds adsorbed onto the cathode was analysed by using a Perkin Elmer Lambda 10 UV/VIS. Absorbance values were given in unit absorbance (UA).

Generated carboxylic acids were monitored by ion-exclusion HPLC, as detailed by Olvera-Vargas et al. [47].

Iron concentration was analysed using a PerkinElmer Optima 8300 ion coupled plasma optical emission spectrometer (ICP-OES). Some samples were analysed after filtration through 0.7 μm glass fiber filters, while the total iron concentration was analysed after mineralization of samples by addition of hydrogen peroxide and nitric acid in a water bath (95 °C).

2.5. Mathematical modelling

A model has been developed in order to monitor the evolution of TOC in the solution during various EAOPs. The software Aquasim has been used [48]. Both sorption and oxidation processes are considered.

First, it is assumed that organics degradation in the electrochemical cell originates only from reaction with hydroxyl radicals (either •OH from homogeneous catalysis during EF or M(•OH) from heterogeneous catalysis at the surface of BDD anode), a strong oxidizing agent and non-selective reagent with a standard reduction potential of E° ($^\bullet OH/H_2O$) = 2.8 V/SHE [21].

Then, the use of the highly porous CS cathode leads to adsorption of HAs onto its surface. The kinetics of sorption from a solution onto an adsorbent has been well explored by Azizian [49]. The author showed that the sorption process obeys the pseudo-second-order model, provided that the initial concentration of solute is not too high (Eq. (6)),

$$\frac{dq}{dt} = k(q_e - q)^2 \tag{6}$$

where q and q_e are the milligrams of HAs sorbed per gram of sorbent at any time and equilibrium, respectively, and k is the pseudo-second-order rate constant of sorption. One can also rewrite Eq. (6) as follows;

$$\frac{d[HA_{ads}]}{dt} = k'\left([HA_{ads}]_{eq} - [HA_{ads}]\right)^2 \tag{7}$$

where k' is the observed pseudo-second-order rate constant ($(mg\,L^{-1})^{-1}\,h^{-1}$) and $[HA_{ads}]$ and $[HA_{ads}]_{eq}$ are the milligrams of carbon of HAs sorbed per litre of solution ($mg\,L^{-1}$) at any time and equilibrium, respectively; i.e.,

$$[HA_{ads}] = q\frac{m_c}{V_{sol}}\eta \tag{8}$$

where m_c is the mass of sorbent (g), V_{sol} (L) is the volume of the solution and η is the mass fraction of carbon in HAs molecules.

Azizian [49] also reported that the pseudo-second-order rate constant of sorption is a function of the initial concentration of solute. During electrolysis, oxidation of organics modifies the total HAs concentration. Thus, it is proposed to express k' as a simple function of the total HAs concentration, as follows,

$$k' = k_{ads}[HA]_{tot} \tag{9}$$

where $[HA]_{tot}$ is the sum of $[HA_{ads}]$ and HAs concentration in the bulk ($[HA_{sol}]$), and k_{ads} is the fitting parameter for the model (h^{-1}).

Therefore, the following Eq. (10) is the general equation for sorption process of HAs onto the CS cathode during the electrolysis,

$$\frac{d[HA_{ads}]}{dt} = k_{ads}[HA]_{tot}\left([HA_{ads}]_{eq} - [HA_{ads}]\right)^2 \tag{10}$$

Additional assumptions took into consideration for the model are discussed in the 'results and discussion' part, according to the observed experimental results.

Calibration of the model was performed by adjusting unknown parameters until the model outputs adequately fit the experimental observations. Three methods were used for the comparison of model results with experimental measurements, the Root Mean Square Error (RMSE) (Eq. (5)), the Modelling Efficiency (ME) (Eq. (6)) and the Index of Agreement (IoA) (Eq. (7)) [50–52]. Unknown parameters were determined by optimizing these three criteria.

$$RMSE = \sqrt{\frac{\Sigma_{i=1}^{K}(y_i - y'_i)^2}{K}} \tag{11}$$

$$ME = 1 - \frac{\Sigma_{i=1}^{K}(y_i - y'_i)^2}{\Sigma_{i=1}^{K}(y_i - y'_M)^2} \tag{12}$$

$$IoA = 1 - \frac{\sum_{i=1}^{K}(y_i - y'_i)^2}{\sum_{i=1}^{K}(|y'_i - y_M| + |y_i - y_M|)^2} \tag{13}$$

where K is the number of observed values, y_i is the single numerically simulated value, y'_i is the corresponding experimentally observed value, y_M is the average of the numerically simulated values.

3. Results and discussion

3.1. Removal of HAs during AO-CS and AO-SS processes

3.1.1. Experimental results

The TOC evolution during the AO-SS process according to the current supply intensity is reported in Fig. 1. More than 99% of TOC removal was reached after 7 h of treatment at 1000 mA. No significant HAs adsorption (<2%) was observed onto the SS cathode. Mineralization kinetics are well fitted ($R^2 > 0.99$) with the pseudo-first-order model (Eq. (13)) (Fig. 1). This is in accordance with Panizza et al. [25]: when the applied current is high or the concentration of the organics is low, organics electrolysis by •OH formed at the surface of the anode (BDD(•OH)) is under mass-transport control [28,36]. Additionally, the decrease of the current intensity from 1000 to 600 and 300 mA reduced pseudo-first order constant by 2.1 and 4.1, respectively. This is attributed to the lower production of •OH at the surface of the BDD anode.

$$\frac{d[TOC]}{dt} = -k_{min\_BDD}[TOC] \tag{14}$$

k_{min_BDD} being the pseudo-first-order rate constant of HAs mineralization at the surface of the BDD anode (h^{-1}).

Higher TOC removal is reached with the AO-BDD process using SS cathode, compared to all other AOPs already investigated for NOM removal from water. For example, Fenton's reaction based process, ozone based process and photocatalysis achieved maximum TOC removal in the range 60–85% [53–55]. There is not any data available in the literature about removal of HAs by EAOPs to compare with.

Interestingly, no change in the UV spectrum of the solution during the treatment by AO-SS was observed (Fig. 2). Moreover, short chain carboxylic acids have not been detected by ion exclusion chromatography (*i.e.* concentrations were below 0.01 mM) during the treatment at 1000 mA. Additional analysis such as Fourier transform infrared spectroscopy should be required to verify that oxidation by-products were not accumulated in the bulk. However, this indicates complete mineralization of organics to CO_2 near the anode surface without accumulation of oxidation by-products in the bulk. This is consistent with theoretical considerations: the high oxygen overpotential of BDD allows the formation of large amounts

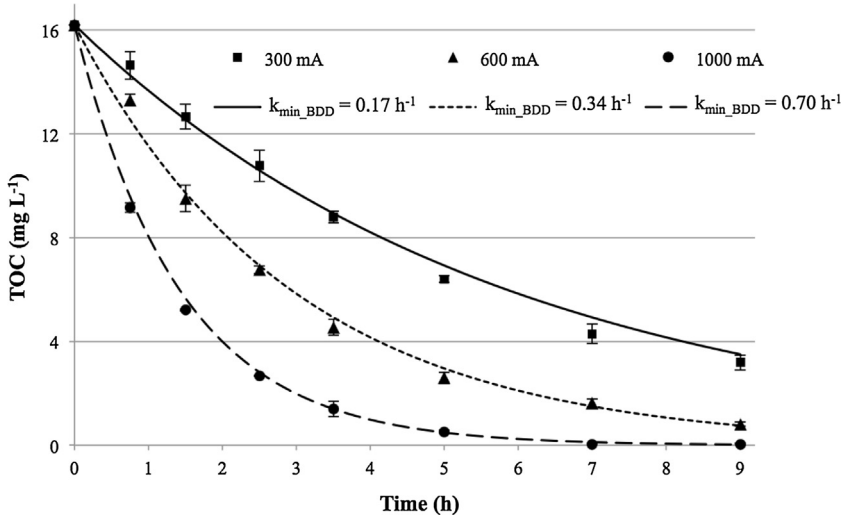

Fig. 1. Evolution of TOC_{sol} during the electrolysis of HAs (TOC_0 = 16.2 mg L^{-1}) in 0.05 M Na_2SO_4 solution by AO-SS process according to the current intensity applied (300–600–1000 mA). Error bars refer to triplicate experiments. Lines report model results.

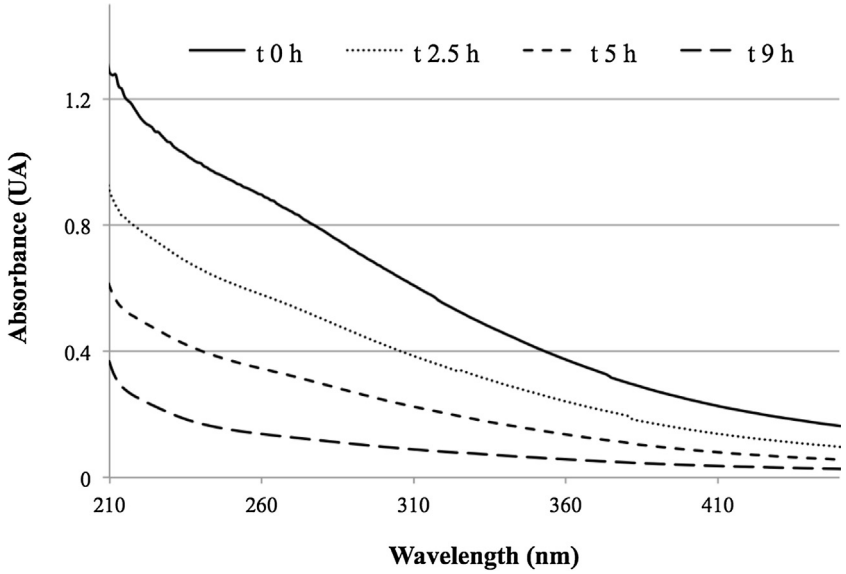

Fig. 2. Evolution of the UV spectrum of HAs (TOC_0 = 16.2 mg L^{-1}) in 0.05 M Na_2SO_4 solution during the treatment by the AO-SS process at 300 mA.

of •OH or physisorbed "active oxygen" at the surface of the anode (BDD(•OH)). This assists the nonselective oxidation of organics and their complete combustion to CO_2 [44,56,57]. Therefore, AO process appears as one of the most effective technique for the complete mineralization of HAs solutions and production of organic-free water. In this lab-scale configuration energy consumption to reach 50% TOC removal was calculated as 2.7, 3.9 and 4.7 kWh (g TOC)$^{-1}$, respectively, at 300 mA, 600 mA and 1000 mA, respectively. The higher energy consumption for high current intensity comes from the increase of secondary reactions (such as H_2 (cathode) and O_2 (anode) evolution), resulting in the decrease of current efficiency.

The evolution of TOC_{sol} and TOC_{ads} during the AO-CS process at 300 mA is reported in Fig. 3. Much lower efficiency was observed for the AO-CS process (59% TOC_{tot} removal after 9 h of treatment), compared to the AO-SS process (80% TOC_{tot} removal after 9 h treatment). This fact can be explained by the adsorption of organic compounds onto the porous CS cathode as it is shown by the continuous increase of TOC_{ads}. This adsorption phenomenon depends on both organic compounds and electrode material characteristics and should be assessed in electrochemical processes using carbonaceous materials. Other methods for desorption of organic compounds could be necessary depending on the nature of compounds studied. There was not any significant decrease of TOC_{ads} during the experiment. Hydroxyl radicals produced at the surface of the BDD anode have very short lifetime, in the range of nanoseconds. Thus, they cannot react with organics adsorbed onto the CS cathode because their lifetime is too low to reach the cathode.

3.1.2. Mathematical modelling

Based on these experimental observations, the proposed model considers only mineralization of HAs in the bulk (Eq. (14)) and HAs sorption onto the CS cathode (Eq. (10)). Production of HAs oxidation by-products (HABPs) is neglected. Therefore, it is assumed that $[HA_{ads}] = TOC_{ads}$ and $[HA_{tot}] = TOC_{tot}$. $[TOC_{ads}]_{eq}$ has been determined by using similar experimental conditions, but without current supply in order to avoid oxidation of organics. The equilibrium has been reached after 1 day with $[TOC_{ads}]_{eq}$ = 6.0 mg L^{-1}. Besides, it has been observed during electrolysis experiments that the adsorption kinetic (parameter k_{ads}) was strongly increased when current intensity is supplied. This indicates that both elec-

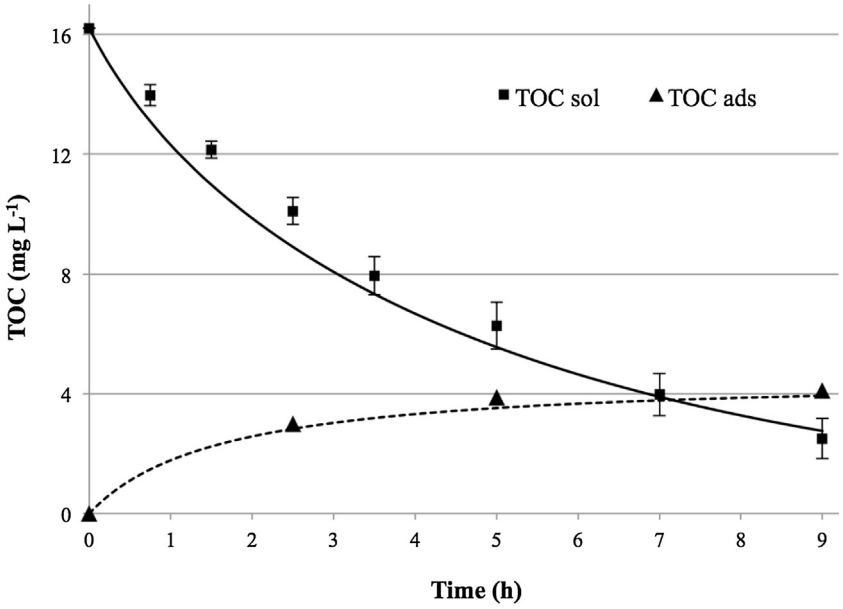

Fig. 3. Evolution of TOC_{sol} and TOC_{ads} during the electrolysis of HAs (TOC_0 = 16.2 mg L^{-1}) in 0.05 M Na_2SO_4 solution by AO-CS process at 300 mA. Symbols report experimental results. Error bars refer to triplicate experiments. Lines report model results.

trostatic and hydrophobic interactions are involved during the sorption process. Therefore, it was not possible to fit the parameter k_{ads} in a separate experiment as oxidation of HAs occurs when current intensity is supplied.

3.2. HAs removal during EF-Pt and EF-BDD processes

3.2.1. Experimental results

The evolution of TOC_{sol} and TOC_{ads} during the EF-Pt process at 300 mA is depicted in Fig. 4. A fast decrease of the TOC_{sol} was observed during the first 40 min of the treatment. It has been simultaneously noticed the adsorption of more than 85% of the initial TOC onto the CS cathode. The enhancement of the adsorption process could be attributed to a complex formation between HAs and iron ions, allowing charge neutralization of HAs. This has been confirmed by iron analysis during the EF-Pt process. After 15 min of treatment, 45% of the iron in the solution was in the fraction >0.7 μm. This indicates the formation of macro complex between iron and HAs. Then, this ratio continuously decreased and reached 26% after 7 h of treatment. This can be attributed to the lower affinity between HABPs and iron ions, leading to lower formation of complex.

In contrast to the AO process, TOC_{ads} decreased from 85% to 22% of the initial TOC (TOC_0) between 0.7 h and 9 h when performing the EF-Pt process. This is explained by the availability of adsorbed organics to oxidation by •OH produced homogeneously in the bulk from Fenton's reaction (Eq. (2)). The main pathway for aromatic organics degradation by •OH is hydroxylation (electrophilic addition) to non-saturated bond or H atom abstraction followed by further oxidation [40,43]. This allows the conversion of HAs into more polar by-products that have low interaction with the CS cathode. Sanly et al. [58] already showed the fragmentation of the hydrophobic fraction of HAs into hydrophilic and slightly hydrophilic compounds during the Fenton process. Therefore, the increase in TOC_{sol} from 8% to 40% of the initial TOC (TOC_0) between 0.7 and 5 h of treatment is ascribed to the accumulation of HABPs in the solution. This is in accordance with the change in the shape of the UV spectrum of the solution during the EF treatment. Particularly, a decrease of the absorbance between 250 nm and 300 nm has been observed. This is typical of aromatic rings breaking and indicates the presence of more hydrophilic organics in the solution. Similar mechanism and rebound effect was observed during the homogeneous photocatalysis (TiO_2/UV) process, due to the initial fast adsorption of HAs onto TiO_2 particles [54].

On the contrary, it has not been observed any significant change in the shape of the UV spectrum of compounds adsorbed onto the CS cathode, compared to the one of the initial solution of HAs. This denotes that compounds adsorbed onto CS cathode can be characterized as low or non-degraded HAs (Fig. 5).

The TOC_{ads} and TOC_{sol} evolution during the EF-BDD process is reported in Fig. 6. Similar removal of TOC_{ads} was observed during EF-BDD and EF-Pt processes between 0.7 and 9 h of treatment. This indicates a similar bulk production of •OH in both processes. This is in accordance with results observed during the AO process with CS cathode, showing that heterogeneous hydroxyl radicals (BDD(•OH)) produced at the surface of the BDD anode cannot contribute to the oxidation of organics adsorbed onto the CS cathode.

After the fast adsorption of HAs, TOC evolution in the solution depends on accumulation of HABPs in the bulk due to oxidation of adsorbed HAs, as well as mineralization of these by-products to CO_2. Thus, the rebound effect of the TOC in the solution during the EF-Pt process is attributed to a higher oxidation rate of adsorbed HAs compared to the mineralization rate of HABP. In contrast, the use of BDD anode (EF-BDD process) instead of Pt anode leads to a much lower rebound effect (Fig. 6). This is due to the accumulation of BDD(•OH) at the surface of the anode, promoting mineralization of HABPs.

3.2.2. Mathematical modelling

On the contrary to the AO process, experimental observations lead to take into consideration two different types of organic compounds: low or non-degraded HAs (HA_{Hob}) that can adsorb onto the CS cathode (HA_{Hob_ads}) and more hydrophilic HABPs without interactions with the CS cathode. Thus, the following conclusions can be drawn:

$$[HA_{ads}] = [HA_{Hob\_ads}] = TOC_{ads},$$

$$[HA_{tot}] = [HA_{Hob}] + TOC_{ads},$$

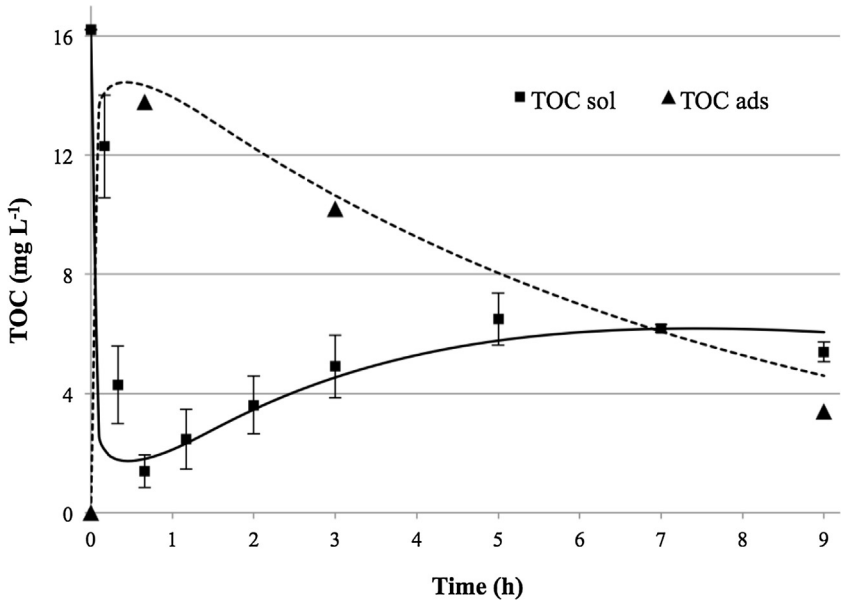

Fig. 4. Evolution of TOC_{sol} and TOC_{ads} during the electrolysis of HAs solution (TOC_0 = 16.2 mg L^{-1}) by EF-Pt process at 300 mA (0.05 M Na_2SO_4; 0.1 mM Fe^{2+}). Symbols report experimental results. Error bars refer to triplicate experiments. Lines report model results.

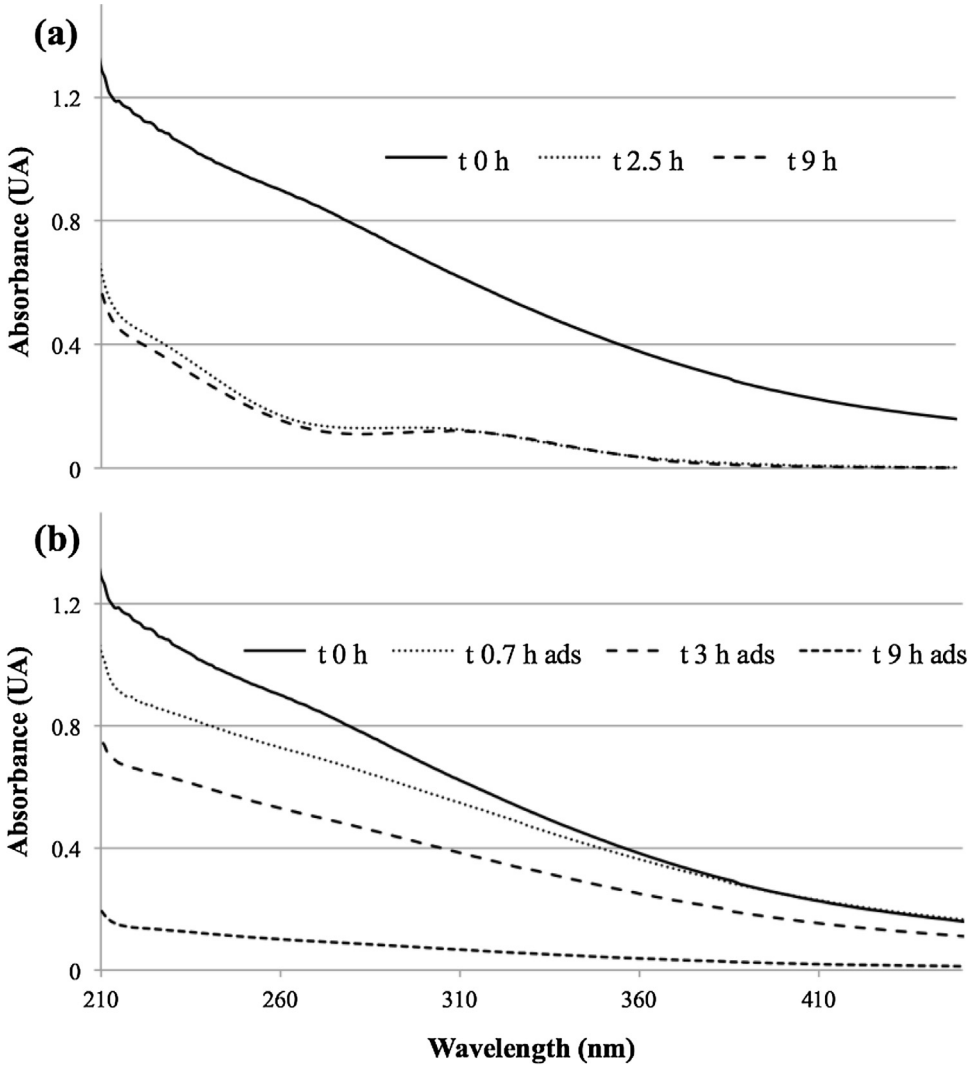

Fig. 5. Evolution of the UV spectrum of organics in the solution (a) and adsorbed onto the carbon sponge cathode (b) during the treatment of HAs solution (TOC_0 = 16.2 mg L^{-1}) by EF-BDD process at 300 mA (0.05 M Na_2SO_4; 0.1 mM Fe^{2+}).

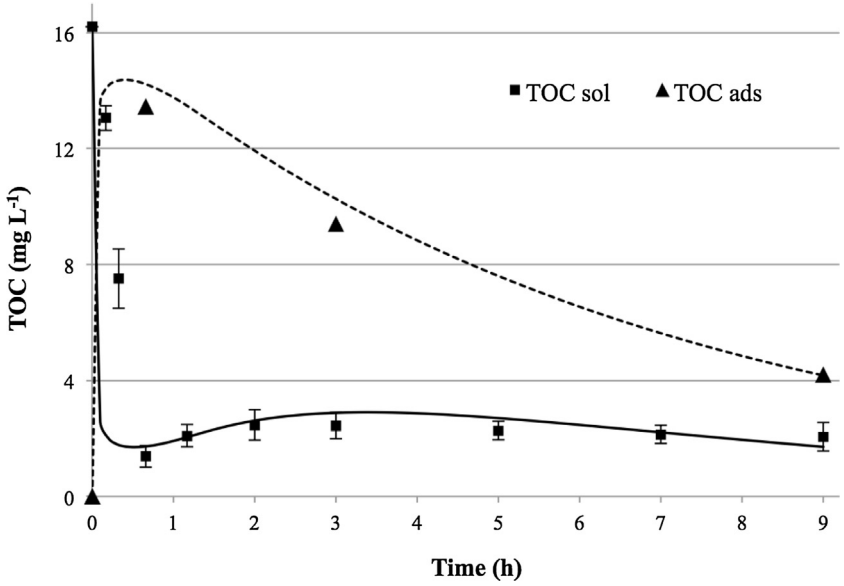

Fig. 6. Evolution of TOC_{sol} and TOC_{ads} during the electrolysis of HAs solution (TOC_0 = 16.2 mg L^{-1}) by EF-BDD process at 300 mA (0.05 M Na_2SO_4; 0.1 mM Fe^{2+}). Symbols report experimental results. Error bars refer to triplicate experiments. Lines report model results.

$TOC_{sol} = [HA_{Hob}] + [HABP]$.

The fast adsorption of a large amount of humic acids during the first 45 min of the process leads to assume that $[HA_{Hob\_ads}]$ at equilibrium ($[HA]_{Hob\_ads\_eq}$) is 16.2 mg L^{-1} (initial concentration of HAs). This is coherent with the following phenomenon. Charge neutralization of HAs and macro complex formation coming from the addition of iron salts increase the potential of adsorption of HAs onto the CS cathode. Therefore, the porosity of the CS electrode (60 pores per inch) allows considering that the specific surface area of the sum of HAs is much lower than the specific surface area of the CS cathode available for adsorption.

As regards to the modelling of oxidation mechanisms, pseudo-first-order reactions are considered for the kinetic model of organics degradation, in accordance with most of literature results investigating the degradation of organic compounds by the EF process [40]. It is also assumed that oxidation of HA_{Hob_ads} leads to the direct release of HABPs into the solution. Processes considered in the model are summarized in the following Petersen matrix (Table 1).

3.3. Discussion about the model

Calibrated parameters have been determined in order to minimize RMSE and optimize ME and IoA. Moreover, a logical approach based on experimental observations and theoretical considerations was followed for the estimation of parameters. Mineralization rate (k_{min_BDD}) during AO oxidation was estimated by results observed with SS cathode, for which adsorption did not occur. Then, a similar k_{min_BDD} was chosen for the AO-CS process since organics removal during AO occurs mainly through heterogeneous catalysis at the surface of the BDD anode, regardless to the cathode material used. Oxidation of HAs by H_2O_2 produced at the CS cathode is neglected, in accordance with its lower standard reduction potential (1.763 E°/V *vs* SHE) compared to •OH (2.80 E°/V *vs* SHE). Since the equilibrium parameter of adsorption of HAs onto the CS cathode was determined in a separated experiment, the remaining parameter k_{ads} has been obtained according to experimental results during electrolysis. Oxidation parameters during the EF process were estimated by taking into consideration a similar k_{HA_ads} for both EF-Pt and EF-BDD process since this parameter is only related to homogeneous catalysis from Fenton's reaction, with low influence of the anode material. Moreover, a higher k_{HABP} for the EF-BDD process compared to the EF-Pt process was chosen due to the of additional generation of BDD(•OH) by heterogeneous catalysis. Finally, adsorption parameters during EF process have been fitted according to experimental results during electrolysis.

These values are all reported in Tables 2 and 3. Good correlation is observed between experimental results and model outputs, indicating the relevance of the modelling approach proposed in this paper.

As regards to the sorption process, the predetermined value of $[HA]_{ads\_eq}$ for the AO-CS process allows fitting well with the evolution of TOC_{ads} during this treatment. The proposed sorption model also fits well with the low TOC_{sol} and high TOC_{ads} concentration reached after 40 min of treatment during the EF-Pt and EF-BDD processes. However, high RMSE as well as low ME and IoA values have been calculated for the evolution of TOC_{sol} during EF-Pt and EF-BDD processes. This is due to the overestimation of the kinetic of TOC_{sol} decrease during the first 40 min of the treatment. Without taking into account experimental points observed at t = 0.17 h and t = 0.33 h, ME values are greatly improved for EF-Pt and EF-BDD (0.994 and 0.997, respectively). Interestingly, the use of a lower k_{ads} parameter did not improve the global model quality. It leads to an underestimation of HAs adsorption rate, since a greater amount of HAs is degraded into HABPs before to be adsorbed. Therefore, the experimental results could only be explained by considering additional mass transfer limitations. Particularly, this could be related to a diffusion/convection mechanism corresponding to the time necessary for the solution to fully penetrate into the porous CS cathode. Indeed, the real CS surface available for HAs adsorption and H_2O_2 production is progressively increasing during the beginning of the process. Further investigations and experimental results would be necessary for the calibration of this process.

Previous models have been developed for EAOPs in order to monitor the degradation of single model organic compounds such as phenol [39] by following the generation of oxidation by-products until total mineralization. However, in a complex mixture of organic compounds such as solution of HAs, alternative model based on a global parameter (TOC, chemical oxygen demand) can be required. Moreover, it is the first time that sorption processes are

Table 1
Petersen matrix of processes taken into account for modelling the evolution of TOC_{sol} and TOC_{ads} during treatment of HAs solution by EF-Pt and EF-BDD.

Process	HA_{Hob}	HA_{Hob_ads}(=TOC_{ads})	HABPs	Min. prod.[a]	Reaction rate (mg L^{-1} h^{-1})
HA_{Hob} adsorption onto CS cathode	−1	1			k_{ads} ([HA_{Hob}] + TOC_{ads})(TOC_{ads_eq}−TOC_{ads})^2
HA_{Hob} conversion into HABPs	−1		1		k_{HA} [HA_{Hob}]
HA_{Hob_ads} conversion into HABPs		−1	1		k_{HAads} [TOC_{ads}]
HABPs mineralization			−1	1	k_{HABP} [HABP]

[a] Mineralization products (CO_2, H_2O, inorganic ions).

Table 2
Calibration of model parameters.

Process (I = 300 mA)	k_{min_BDD} (h^{-1})	k_{ads} (h^{-1})	$[HA]_{ads,eq}$ (mg L^{-1})	k_{HA} (h^{-1})	k_{HAads} (h^{-1})	k_{HABP} (h^{-1})
AO-SS	0.17	0	0	–		
AO-CS	0.16	0.005	6.0			
EF-Pt	–	0.8	16.2	0.14	0.14	0.13
EF-BDD		0.8	16.2	0.24	0.15	0.50

Table 3
Comparison of model outputs with experimental measurements (Root mean square error, model efficiency and index of agreement methods).

Process(I = 300 mA)	RMSE		ME		IoA	
	TOC sol	TOC ads	TOC sol	TOC ads	TOC sol	TOC ads
AO-SS	0.366	–	0.993	–	0.998	–
AO-CS	0.752	0.216	0.973	0.982	0.993	0.996
EF-Pt	3.69	0.345	0.336	0.996	0.847	0.999
EF-BDD	4.36	0.457	0.191	0.992	0.832	0.998

took into consideration for TOC removal modelling during EAOPs. The next step would be to combine this model with previously research works modelling the generation and the role of hydroxyl radicals according to operating conditions [25,59–61].

4. Conclusions

This paper reports for the first time the removal of HAs by various EAOPs. The following main results and conclusions could be drawn from results obtained:

- More than 99% of TOC of initial solution (16.2 mg L^{-1}) was removed after 7 h of treatment at 1000 mA using AO process with BDD anode and SS cathode. This process generates low amount of intermediates and lead to rapid mineralization of organics to CO_2.
- The use of CS material as cathode leads to significant HAs sorption onto its surface. This results in a lower amount of HAs oxidised during the AO process. Addition of iron during the EF process strongly enhances both kinetic and capacity of HAs adsorption onto CS cathode.
- Hydroxyl radicals produced from the Fenton's reaction can oxidize organics adsorbed onto the cathode, as they are produced in a homogeneous way in the bulk. This results in the release of hydrophilic HABPs in the solution.
- The mineralization to CO_2 of HABPs is much more efficient using BDD anode, compared to Pt anode, due to its higher catalytic activity for heterogeneous $^{\bullet}OH$ production.

The proposed model allows monitoring TOC_{sol} and TOC_{ads} evolution during AO-SS, AO-CS, EF-Pt and EF-BDD process. It takes into account both sorption and oxidation processes as well as two different types of organics (low or non-degraded HAs and hydrophilic HABPs). However, the reliability of this model should be validated with different experimental conditions, such as various initial concentrations, nature of organics, current intensity. Moreover, it has been highlighted that diffusion/convection of the solution inside the CS cathode should also be considered for the assessment of the catalytic activity of this material for H_2O_2 generation.

To conclude, EAOPs are promising processes for the production of high quality organic-free water, particularly when BDD anode is used. As regards to drinking water treatment plant issues, it would be interesting to evaluate the evolution of the potential of formation of disinfection by-products in parallel with energy consumption optimization.

Acknowledgements

Clément Trellu would like to acknowledge the Education, Audiovisual and Culture Executive Agency of the European Commission for financial support. Clément Trellu is a Doctoral research fellow of the Erasmus Mundus Joint Doctorate programme ETeCoS^3 (Environmental Technologies for Contaminated Solids, Soils and Sediments) under the grant agreement FPA no. 2010-0009.

Bibliography

[1] M. Schnitzer, S.U. Khan, Soil Organic Matter, Elsevier Science Publishers B.V., 1978, 2016.
[2] F.J. Stevenson, Humus Chemistry: Genesis, Composition, Reactions, Wiley Interscience, New York, 1982.
[3] G. Hua, D.A. Reckhow, Characterization of disinfection byproduct precursors based on hydrophobicity and molecular size, Environ. Sci. Technol. 41 (2007) 3309–3315, http://dx.doi.org/10.1021/es062178c.
[4] V.K. Sharma, R. Zboril, T.J. McDonald, Formation and toxicity of brominated disinfection byproducts during chlorination and chloramination of water: a review, J. Environ. Sci. Health Part B 49 (2014) 212–228, http://dx.doi.org/10.1080/03601234.2014.858576.
[5] U. von Gunten, A. Driedger, H. Gallard, E. Salhi, By-products formation during drinking water disinfection: a tool to assess disinfection efficiency? Water Res. 35 (2001) 2095–2099, http://dx.doi.org/10.1016/S0043-1354(01)00051-3.
[6] A. Matilainen, M. Vepsalainen, M. Sillanpaa, Natural organic matter removal by coagulation during drinking water treatment: a review, Adv. Colloid Interface Sci. 159 (2010) 189–197, http://dx.doi.org/10.1016/j.cis.2010.06.007.
[7] J.A. Leenheer, J.-P. Croué, Characterizing aquatic dissolved organic matter, Environ. Sci. Technol. 37 (2003) 18A–26A.

[8] A. Matilainen, M. Sillanpaa, Removal of natural organic matter from drinking water by advanced oxidation processes, Chemosphere 80 (2010) 351–365, http://dx.doi.org/10.1016/j.chemosphere.2010.04.067.
[9] S. Valencia, J.M. Marin, G. Restrepo, F.H. Frimmel, Evaluation of natural organic matter changes from Lake Hohloh by three-dimensional excitation-emission matrix fluorescence spectroscopy during TiO2/UV process, Water Res. 51 (2014) 124–133, http://dx.doi.org/10.1016/j.watres.2013.12.019.
[10] P. Jin, X. Jin, V.A. Bjerkelund, S.W. Østerhus, X.C. Wang, L. Yang, A study on the reactivity characteristics of dissolved effluent organic matter (EfOM) from municipal wastewater treatment plant during ozonation, Water Res. 88 (2016) 643–652, http://dx.doi.org/10.1016/j.watres.2015.10.060.
[11] P. Sathishkumar, R.V. Mangalaraja, S. Anandan, Review on the recent improvements in sonochemical and combined sonochemical oxidation processes – A powerful tool for destruction of environmental contaminants, Renew. Sustainable Energy Rev. 55 (2016) 426–454, http://dx.doi.org/10.1016/j.rser.2015.10.139.
[12] H.R. Sindelar, M.T. Brown, T.H. Boyer, Evaluating UV/H2O2, UV/percarbonate, and UV/perborate for natural organic matter reduction from alternative water sources, Chemosphere 105 (2014) 112–118, http://dx.doi.org/10.1016/j.chemosphere.2013.12.040.
[13] O. Ganzenko, D. Huguenot, E.D. van Hullebusch, G. Esposito, M.A. Oturan, Electrochemical advanced oxidation and biological processes for wastewater treatment: a review of the combined approaches, Environ. Sci. Pollut. Res. (2014) 1–32, http://dx.doi.org/10.1007/s11356-014-2770-6.
[14] H. Lin, J. Wu, H. Zhang, Degradation of bisphenol A in aqueous solution by a novel electro/Fe^{3+}/peroxydisulfate process, Sep. Purif. Technol. 117 (2013) 18–23, http://dx.doi.org/10.1016/j.seppur.2013.04.026.
[15] E. Brillas, C.A. Subba, Decontamination of wastewaters containing synthetic organic dyes by electrochemical methods. An updated review, Appl. Catal. B 166–167 (2015) 603–643, http://dx.doi.org/10.1016/j.apcatb.2014.11.016.
[16] I. Sirés, E. Brillas, M.A. Oturan, M.A. Rodrigo, M. Panizza, Electrochemical advanced oxidation processes: today and tomorrow. A review, Environ. Sci. Pollut. Res. 21 (2014) 8336–8367, http://dx.doi.org/10.1007/s11356-014-2783-1.
[17] S. Vasudevan, M.A. Oturan, Electrochemistry: as cause and cure in water pollution—an overview, Environ. Chem. Lett. 12 (2014) 97–108, http://dx.doi.org/10.1007/s10311-013-0434-2.
[18] E. Isarain-Chávez, C. de la Rosa, L.A. Godínez, E. Brillas, J.M. Peralta-Hernández, Comparative study of electrochemical water treatment processes for a tannery wastewater effluent, J. Electroanal. Chem. 713 (2014) 62–69, http://dx.doi.org/10.1016/j.jelechem.2013.11.016.
[19] N. Oturan, E.D. van Hullebusch, H. Zhang, L. Mazeas, H. Budzinski, K. Le Menach, et al., Occurrence and removal of organic micropollutants in landfill leachates treated by electrochemical advanced oxidation processes, Environ. Sci. Technol. 49 (2015) 12187–12196, http://dx.doi.org/10.1021/acs.est.5b02809.
[20] A.N.S. Rao, V.T. Venkatarangaiah, Metal oxide-coated anodes in wastewater treatment, Environ. Sci. Pollut. Res. 21 (2013) 3197–3217, http://dx.doi.org/10.1007/s11356-013-2313-6.
[21] W.M. Latimer, Oxidation Potentials, Prentice-Hall, 1952, 2016.
[22] B. Balci, N. Oturan, R. Cherrier, M.A. Oturan, Degradation of atrazine in aqueous medium by electrocatalytically generated hydroxyl radicals. A kinetic and mechanistic study, Water Res. 43 (2009) 1924–1934, http://dx.doi.org/10.1016/j.watres.2009.01.021.
[23] A. Dirany, I. Sirés, N. Oturan, M.A. Oturan, Electrochemical abatement of the antibiotic sulfamethoxazole from water, Chemosphere 81 (2010) 594–602, http://dx.doi.org/10.1016/j.chemosphere.2010.08.032.
[24] M.A. Oturan, An ecologically effective water treatment technique using electrochemically generated hydroxyl radicals for *in situ* destruction of organic pollutants: application to herbicide 2,4-D, J. Appl. Electrochem. 30 (2000) 475–482, http://dx.doi.org/10.1023/A:1003994428571.
[25] M. Panizza, P.A. Michaud, G. Cerisola, C. Comninellis, Anodic oxidation of 2-naphthol at boron-doped diamond electrodes, J. Electroanal. Chem. 507 (2001) 206–214, http://dx.doi.org/10.1016/S0022-0728(01)00398-9.
[26] M.A. Rodrigo, P.A. Michaud, I. Duo, M. Panizza, G. Cerisola, C. Comninellis, Oxidation of 4-chlorophenol at boron-doped diamond electrode for wastewater treatment, J. Electrochem. Soc. 148 (2001) D60–D64, http://dx.doi.org/10.1149/1.1362545.
[27] A. Thiam, M. Zhou, E. Brillas, I. Sirés, Two-step mineralization of Tartrazine solutions: study of parameters and by-products during the coupling of electrocoagulation with electrochemical advanced oxidation processes, Appl. Catal. B 150–151 (2014) 116–125, http://dx.doi.org/10.1016/j.apcatb.2013.12.011.
[28] C.A. Martínez-Huitle, S. Ferro, Electrochemical oxidation of organic pollutants for the wastewater treatment: direct and indirect processes, Chem. Soc. Rev. 35 (2006) 1324–1340, http://dx.doi.org/10.1039/B517632H.
[29] C.A. Martínez-Huitle, M.A. Rodrigo, I. Sirés, O. Scialdone, Single and coupled electrochemical processes and reactors for the abatement of organic water pollutants: a critical review, Chem. Rev. 115 (2015) 13362–13407, http://dx.doi.org/10.1021/acs.chemrev.5b00361.
[30] M.E. Lindsey, M.A. Tarr, Inhibition of hydroxyl radical reaction with aromatics by dissolved natural organic matter, Environ. Sci. Technol. 34 (2000) 444–449, http://dx.doi.org/10.1021/es990457c.
[31] S.K. Hong, M. Elimelech, Chemical and physical aspects of natural organic matter (NOM) fouling of nanofiltration membranes, J. Membr. Sci. 132 (1997) 159–181, http://dx.doi.org/10.1016/S0376-7388(97)00060-4.
[32] N.H. Lee, G. Amy, J.P. Croue, H. Buisson, Identification and understanding of fouling in low-pressure membrane (MF/UF) filtration by natural organic matter (NOM), Water Res. 38 (2004) 4511–4523, http://dx.doi.org/10.1016/j.watres.2004.08.013.
[33] P. Westerhoff, S.P. Mezyk, W.J. Cooper, D. Minakata, Electron pulse radiolysis determination of hydroxyl radical rate constants with Suwannee river fulvic acid and other dissolved organic matter isolates, Environ. Sci. Technol. 41 (2007) 4640–4646, http://dx.doi.org/10.1021/es062529n.
[34] E. Mousset, N. Oturan, E.D. van Hullebusch, G. Guibaud, G. Esposito, M.A. Oturan, Treatment of synthetic soil washing solutions containing phenanthrene and cyclodextrin by electro-oxidation. Influence of anode materials on toxicity removal and biodegradability enhancement, Appl. Catal. B 160–161 (2014) 666–675, http://dx.doi.org/10.1016/j.apcatb.2014.06.018.
[35] C. Comninellis, Electrocatalysis in the electrochemical conversion/combustion of organic pollutants for waste-water treatment, Electrochim. Acta 39 (1994) 1857–1862, http://dx.doi.org/10.1016/0013-4686(94)85175-1.
[36] M. Panizza, G. Cerisola, Direct and mediated anodic oxidation of organic pollutants, Chem. Rev. 109 (2009) 6541–6569, http://dx.doi.org/10.1021/cr9001319.
[37] A. Özcan, Y. Şahin, M.A. Oturan, Removal of propham from water by using electro-Fenton technology: kinetics and mechanism, Chemosphere 73 (2008) 737–744, http://dx.doi.org/10.1016/j.chemosphere.2008.06.027.
[38] H. Zhang, C. Fei, D. Zhang, F. Tang, Degradation of 4-nitrophenol in aqueous medium by electro-Fenton method, J. Hazard. Mater. 145 (2007) 227–232, http://dx.doi.org/10.1016/j.jhazmat.2006.11.016.
[39] E. Mousset, L. Frunzo, G. Esposito, E.D. van Hullebusch, N. Oturan, M.A. Oturan, A complete phenol oxidation pathway obtained during electro-Fenton treatment and validated by a kinetic model study, Appl. Catal. B-Environ. 180 (2016) 189–198, http://dx.doi.org/10.1016/j.apcatb.2015.06.014.
[40] E. Brillas, I. Sirés, M.A. Oturan, Electro-Fenton process and related electrochemical technologies based on Fenton's reaction chemistry, Chem. Rev. 109 (2009) 6570–6631, http://dx.doi.org/10.1021/cr900136g.
[41] N. Oturan, M. Zhou, M.A. Oturan, Metomyl degradation by electro-Fenton and electro-Fenton-like processes: a kinetics study of the effect of the nature and concentration of some transition metal ions as catalyst, J. Phys. Chem. A 114 (2010) 10605–10611, http://dx.doi.org/10.1021/jp1062836.
[42] J.J. Aaron, M.A. Oturan, New photochemical and electrochemical methods for the degradation of pesticides in aqueous media. Environmental applications, Turk. J. Chem. 25 (2001) 509–520.
[43] M.A. Oturan, J.J. Aaron, Advanced oxidation processes in water/wastewater treatment: principles and applications. a review, Crit. Rev. Environ. Sci. Technol. 44 (2014) 2577–2641, http://dx.doi.org/10.1080/10643389.2013.829765.
[44] A. Ozcan, Y. Sahin, A.S. Koparal, M.A. Oturan, A comparative study on the efficiency of electro-Fenton process in the removal of propham from water, Appl. Catal. B-Environ. 89 (2009) 620–626, http://dx.doi.org/10.1016/j.apcatb.2009.01.022.
[45] H. Arai, M. Arai, A. Sakumoto, Exhaustive degradation of humic acid in water by simultaneous application of radiation and ozone, Water Res. 20 (1986) 885–891, http://dx.doi.org/10.1016/0043-1354(86)90177-6.
[46] A. Baglieri, A. Ioppolo, M. Nègre, M. Gennari, A method for isolating soil organic matter after the extraction of humic and fulvic acids, Org. Geochem. 38 (2007) 140–150, http://dx.doi.org/10.1016/j.orggeochem.2006.07.007.
[47] H. Olvera-Vargas, N. Oturan, E. Brillas, D. Buisson, G. Esposito, M.A. Oturan, Electrochemical advanced oxidation for cold incineration of the pharmaceutical ranitidine: mineralization pathway and toxicity evolution, Chemosphere 117 (2014) 644–651, http://dx.doi.org/10.1016/j.chemosphere.2014.09.084.
[48] P. Reichert, Design techniques of a computer program for the identification of processes and the simulation of water quality in aquatic systems, Environ. Softw. 10 (1995) 199–210, http://dx.doi.org/10.1016/0266-9838(95)00010-I.
[49] S. Azizian, Kinetic models of sorption: a theoretical analysis, J. Colloid Interface Sci. 276 (2004) 47–52, http://dx.doi.org/10.1016/j.jcis.2004.03.048.
[50] G. Esposito, L. Frunzo, A. Panico, F. Pirozzi, Model calibration and validation for OFMSW and sewage sludge co-digestion reactors, Waste Manage. 31 (2011) 2527–2535, http://dx.doi.org/10.1016/j.wasman.2011.07.024.
[51] H. Hauduc, M.B. Neumann, D. Muschalla, V. Gamerith, S. Gillot, P.A. Vanrolleghem, Efficiency criteria for environmental model quality assessment: a review and its application to wastewater treatment, Environ. Model. Softw. 68 (2015) 196–204, http://dx.doi.org/10.1016/j.envsoft.2015.02.004.
[52] A. Panico, G. d'Antonio, G. Esposito, L. Frunzo, P. Iodice, F. Pirozzi, The effect of substrate-bulk interaction on hydrolysis modeling in anaerobic digestion process, Sustainability 6 (2014) 8348–8363, http://dx.doi.org/10.3390/su6128348.
[53] M.A. Alsheyab, A.H. Muñoz, Reducing the formation of trihalomethanes (THMs) by ozone combined with hydrogen peroxide (H2O2/O3), Desalination 194 (2006) 121–126, http://dx.doi.org/10.1016/j.desal.2005.10.028.
[54] X. Huang, M. Leal, Q. Li, Degradation of natural organic matter by TiO2 photocatalytic oxidation and its effect on fouling of low-pressure membranes, Water Res. 42 (2008) 1142–1150, http://dx.doi.org/10.1016/j.watres.2007.08.030.
[55] H. Katsumata, M. Sada, S. Kaneco, T. Suzuki, K. Ohta, Y. Yobiko, Humic acid degradation in aqueous solution by the photo-Fenton process, Chem. Eng. J. 137 (2008) 225–230, http://dx.doi.org/10.1016/j.cej.2007.04.019.

[56] M.A. Rodrigo, P. Cañizares, A. Sánchez-Carretero, C. Sáez, Use of conductive-diamond electrochemical oxidation for wastewater treatment, Catal. Today 151 (2010) 173–177, http://dx.doi.org/10.1016/j.cattod.2010.01.058.
[57] A.M. Sales Solano, C.K. Costa de Araujo, J.V. de Melo, J.M. Peralta-Hernandez, D.R. da Silva, C.A. Martinez-Huitle, Decontamination of real textile industrial effluent by strong oxidant species electrogenerated on diamond electrode: viability and disadvantages of this electrochemical technology, Appl. Catal. B 130 (2013) 112–120, http://dx.doi.org/10.1016/j.apcatb.2012.10.023.
[58] Sanly, M. Lim, K. Chiang, R. Amal, R. Fabris, C. Chow, et al., A study on the removal of humic acid using advanced oxidation processes, Sep. Sci. Technol. 42 (2007) 1391–1404, http://dx.doi.org/10.1080/01496390701289799.
[59] H. Liu, X.Z. Li, Y.J. Leng, C. Wang, Kinetic modeling of electro-Fenton reaction in aqueous solution, Water Res. 41 (2007) 1161–1167, http://dx.doi.org/10.1016/j.watres.2006.12.006.
[60] S. Qiu, D. He, J. Ma, T. Liu, T.D. Waite, Kinetic modeling of the electro-fenton process: quantification of reactive oxygen species generation, Electrochim. Acta 176 (2015) 51–58, http://dx.doi.org/10.1016/j.electacta.2015.06.103.
[61] K. Groenen-Serrano, E. Weiss-Hortala, A. Savall, P. Spiteri, Role of hydroxyl radicals during the competitive electrooxidation of organic compounds on a boron-doped diamond anode, Electrocatalysis 4 (2013) 346–352, http://dx.doi.org/10.1007/s12678-013-0150-5.